Liver Tumour Movement Modelling for Laparoscopic Surgery Purposes

Monika Bugdol, *Silesian University of Technology*

Abstract

The fast growing popularity of minimally invasive surgery is the cause of development of computer systems that are helpful tools during endoscopic procedures.

In the paper a liver deformation model has been presented including the tumour movement inside the organ. The model is an answer to the need of better visualization during laparoscopic surgery. A solution to this issue should be both fast and accurate. Existing solutions to the problem of internal organ deflection were discussed.

The proposed model is an extension of a previously introduced liver deflection model [11], which has been enriched by calculating the movement of liver tissue layers.

Main assumptions of the model have been specified. Essential mathematical transformations have been discussed and a visualization suggestion has been mentioned. The correctness of the new model has been verified using US images of a liver with and without foreign tissue inside, imitating a tumour. There are pictures included in the paper which enable the visual comparison of the real deformation with the one calculated using the new model. Further research matters were briefly described.

1. Introduction

Human health and treatment methods are two of the main research directions. Proper development and functioning of the organism are absolute priorities for many people. Thanks to the technological progress minimally invasive surgery evolved, which qualities are difficult to overestimate. Smaller incision and, as a result, less pain, shorter recovery time and almost invisible post-operative scar are for the patient the most important factors pointing to the benefits of laparoscopic surgery. Moreover, far less bleeding (comparing to conventional surgery) reduces the risk of a haemorrhage. Furthermore, an infection is also much less probable.

Unfortunately, this technology has a drawback, which is insufficient visibility inside the body during surgery. The current solution is to use a camera as one of the tools. However, the picture from such a camera is two-dimensional and covers a relatively narrow scope. In addition, the lack of a proper perspective often makes it difficult or even impossible to assess correctly the exact location of the tools.

These disadvantages are the reason for which attempts are made to establish a system whose task would be to aid minimally invasive surgery paying special attention to extending the possibilities of visualization before and during a surgery. On the basis of CT images an individual model of the patient's abdominal cavity will be constructed. This model, however, is static, when in fact the shapes of internal organs change under the influence of the touch and pressure of laparoscopic tools. The organ surface deformation results in the movement of tumours inside them. A surgeon performing the operation needs to know the exact location of the overgrowth in order to cut as small part of the organ as possible while removing the entire tumour without breaking its structure.

An algorithm estimating the internal organ layer movement is expected to be both very efficient, so that real-time modelling is possible and realistic [1]. Many methods have been implemented to simulate soft tissue deformations: spring-mass models [2], free form deformations [3], various finite element methods (FEM) [[4], [5] [6]] and combinations of the finite element method with other methods like linear [7] or non-linear elasticity [1]. The FEM method is very popular because of its high accuracy in organ deformations, yet it is very time-consuming. Numerous attempts have been made to lower the computational cost of FEM, nonetheless the insufficient efficiency still remains an unsolved problem of this algorithm [8], [9], [10]].

While elaborating the model conditions of a real minimally invasive surgery were assumed - the abdomen is considered being filled with carbon dioxide after insufflation, the liver lies naturally on the stomach and is linked to the diaphragm by the coronary ligament.

2. Mathematical Model of the Liver

The model of tumour movement during liver deformation under the influence of tool pressure presented in the paper is an extension of the liver surface deflection model discussed in [11]. The main issue is to develop a fast and at the same time precise method to calculate the new position of foreign tissue in relation to the current organ shape and the moving trocar.

The organ shape after deformation is described in [11] using a spline curve *C(t)*, consisting of two Bézier curves of degree three, which is calculated on the basis of two space points: the point on the liver surface, that is touched by the tool and the point, at which the tool tip is situated at the moment.

Let there be given: $X = (x_1, x_2, x_3)$ – the point on the liver surface, at which the tool tip touches the organ, $\vec{N} = [n_1, n_2, n_3]$ – the surface normal of the plane tangential to the liver surface at point *X*, $U = (u_1, u_2, u_3)$ – the point at which the tool tip is at the moment and $W = (w_1, w_2, w_3)$ – the point inside the liver whose movement is being estimated (Fig.1).

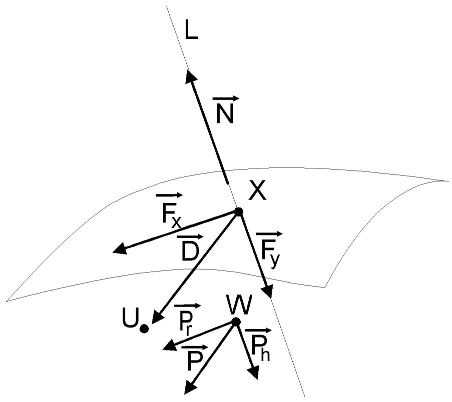

Fig.1. Liver surface and vector system scheme

The tumour inside the organ is considered as a solid object. Its new position is estimated by finding the displacement of three fixed points. This serves as a basis for the translation and rotation of all points of the liver. The first fixed point is the point of the liver closest to the deflected surface. The second one is the place at which the line containing point *X* and the mass center of the tumour crosses the external excrescence layer. The third one is a point on the tumour surface which is distant from the first fixed point by half the tumour radius in the direction of point *X*.

In order to simplify the notation the displacement vector *D* is introduced:

$$\vec{D} = [U - X] = [d_1, d_2, d_3], \tag{1}$$

and line *L* which is parallel to vector *N* and crosses point *X*:

$$L := \begin{cases} x = x_1 + n_1 \cdot t \\ y = x_2 + n_2 \cdot t \quad , t \in \Re \\ z = x_3 + n_3 \cdot t \end{cases}. \tag{2}$$

Vector *D* can be unequivocally written as a sum of two vectors: F_x – a vector parallel to *N* and F_y – a vector perpendicular to *N*:

$$\vec{F}_x = \vec{D} \cdot \sin\Theta, \tag{3}$$

$$\vec{F}_y = \vec{D} \cdot \cos\Theta, \tag{4}$$

where **Θ** is the angle between the normal vector *N* and the displacement vector *D*, so:

$$\vec{F}_y \| \vec{N} \Rightarrow \left(\angle\left(\vec{D}, \vec{F}_y\right) = \angle\left(\vec{D}, \vec{N}\right)\right). \tag{5}$$

Using the definition of the cross product it can be noted, that:

$$|N \times D| = |N| \cdot |D| \cdot \sin\Theta, \tag{6}$$

so after transformation:

$$\sin\Theta = \frac{|N \times D|}{|N| \cdot |D|}. \tag{7}$$

Substituting (11) into (7) the following equation is obtained:

$$\vec{F}_x = \vec{D} \cdot \frac{|N \times D|}{|N| \cdot |D|}. \tag{8}$$

Analogically a transformation of the dot product definition results in:

$$\cos\Theta = \frac{\vec{N} \circ \vec{D}}{|N| \cdot |D|}, \tag{9}$$

and then, substituting (13) into (8):

$$\vec{F}_y = \vec{D} \cdot \frac{\vec{N} \circ \vec{D}}{|N| \cdot |D|}. \tag{10}$$

The movement is a superposition of location change P_h in a direction parallel to the normal vector and P_r, which is perpendicular to P_h. Vector P_r is a product of vector *S*, representing the position change of the projection of point *W* on line *L* and the coefficient **φ1**, which depends on the distance *r* of that point from its projection:

$$\vec{P}_r = \vec{S} \cdot \phi_1(r), \tag{11}$$

where:

$$\phi_1(r) = 1 - \frac{r}{R}. \tag{12}$$

On the basis of the curve, calculated in [11], it has been noticed, that the deformation range *R* of the liver surface is about three times the deflection depth:

$$R \approx 3 \cdot \left|F_y\right|. \tag{13}$$

whereas the distance *r* of point *W* from line *L* is expressed by the formula:

$$r = \left[\frac{n_2}{p}(w_3 - x_3) - \frac{n_3}{p}(w_2 - x_2), \right.$$
$$\frac{n_3}{p}(w_1 - x_1) - \frac{n_1}{p}(w_3 - x_3), \qquad (14)$$
$$\left. \frac{n_1}{p}(w_2 - x_2) - \frac{n_2}{p}(w_1 - x_1) \right]$$

where:

$$p = \sqrt{n_1^2 + n_2^2 + n_3^2}\,. \qquad (15)$$

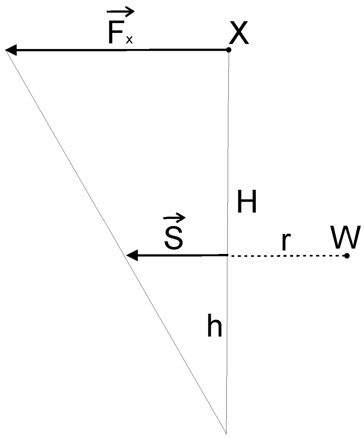

Fig.2. Projection of point *W* on line *L* being translated by vector *S*

According to Fig.2. the following proportion can be noted:

$$\frac{\vec{F}_x}{H} = \frac{\vec{S}}{h}, \qquad (16)$$

consequently vector S is given as:

$$\vec{S} = \frac{h \cdot \vec{F}_x}{H}. \qquad (17)$$

Ultrasound examinations carried out within the confines of the conducted experiment proved that:

$$H \approx |F_y| \cdot 4. \qquad (18)$$

From Fig.2. the following dependency can be noticed:

$$h = H - \sqrt{|(W - X)|^2 - r^2}\,, \qquad (19)$$

thus:

$$\vec{S} = \frac{\left(H - \sqrt{|(W - X)|^2 - r^2} \right) \cdot \vec{F}_x}{H}. \qquad (20)$$

Vector P_h is the product of the coefficient **φ_2,** describing the influence of distance l of point W from the liver surface, the deflection function $\tilde{h}(r)$ and the normalized vector D:

$$\vec{P}_h = \phi_2(l) \cdot \frac{\tilde{h}(r)}{|D|} \cdot \vec{D}, \qquad (21)$$

where:

$$\phi_2(l) = 1 - \frac{l}{H}. \qquad (22)$$

The value of the deflection function depends on radius R and the liver surface deflection Q of a curve for the value R=1, which has been tabuled with the step of 0,001 to shorten the algorithm execution time:

$$\tilde{h}(r) = R \cdot Q\left(\frac{R - r}{R} \right). \qquad (23)$$

The displacement of point P is therefore equal to:

$$\vec{P} = \vec{P}_r + \vec{P}_h. \qquad (24)$$

3. Results

Figures 3 and 5 present liver ultrasound images with the tumour outlined with a white dashed line, at the moment of the laparoscopic tool touching the organ surface. In figures 4 and 6 there are liver ultrasound images with the foreign tissue displacement and the organ deflection, estimated using the model, outlined with a white dashed line.

Three pig liver have been tested. The model error was calculated as the greatest distance between the shape estimated by the model and the real shape of the deflected surface or the moving tumour. The width of the ultrasound head used to perform the imaging is 42 mm. Assessment of that value enabled the estimation of the maximum error of the model, which in the case of test images was 1.8 mm for tumour movement and 3 mm for surface deformation.

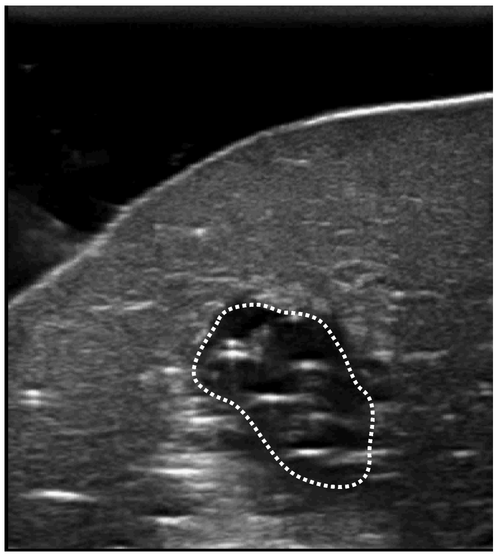

Fig.3. The tumour contour while the tool touches the liver surface

4. Further Research

It is planned to supplement the model with the liver surface shape and tumour displacement description in case of tissue disruption using a tool of a diameter greater than 2 mm. The time of algorithm execution will be estimated. In case of an unsatisfactory result efforts will be made to minimize the computational cost.

Fig.4. The tumour contour and liver deformation while deflecting the liver surface, estimated with the model

Fig.5. The tumour contour while the tool touches the liver surface

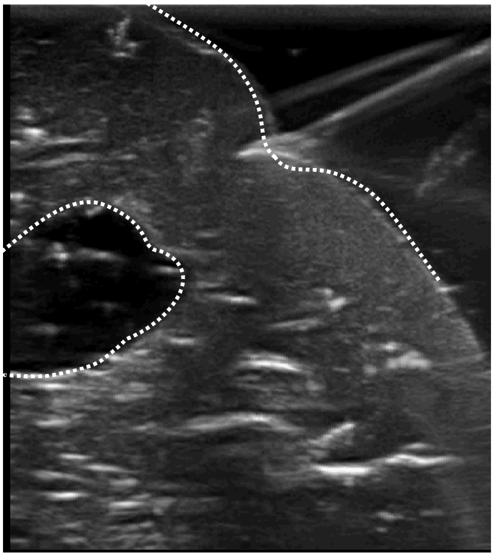

Fig.6. The tumour contour and liver deformation while deflecting the liver surface, estimated with the model

Bibliography

[1] Picinbono G.; Delingette H.; Ayache N.: Nonlinear and Anisotropic Elastic Soft Tissue Models for Medical Simulation, IEEE International Conference on Robotics and Automation 2:1370–1375

[2] Boux de Casson F.; Laugier C.: Modelling the Dynamics of a Human Liver for a Minimally Invasive Surgery Simulator, In MICCAI'99:1156-1165

[3] Basdogan C.; Ho M.; Srinivasan S.; Small D.; Dawson S. L.: Force Interaction in Laparoscopic Simulation: Haptic Rendering Soft Tissues, In MMVR'6:28-31

[4] Bro-Nielsen M.; Cotin S.: Real-Time Volumetric Deformable Models for Surgery Simulation Using Finite Elements and Condensation, In Eurographics'96:57-66

[5] Cotin S.; Delingette H.; Ayache N.: Real-Time Elastic Deformations of Soft Tissues for Surgery Simulation, IEEE Transactions On Visualization and Computer Graphics 5:62-73

[6] Cotin S.; Delingette H.; Ayache N.: A Hybryd Elastic Model for Real-Time Cutting, Deformations and Force Feedback for Surgery Training and Simulation, The Visual Computer 16:437-452

[7] Debunne G.; Desbrun M.; Barr A.; Cani M.-P.: Interactive Multiresolution Animation of Deformable Models, In CAS'99

[8] Muller M.; Dorsey J.; McMillan L.; Jagnow R.; Cutler B.: Stable Real-Time Deformations, In ACM SIGGRAPH:49-54

[9] Nakaguchi T.; Tagaya M.; Tamura N.; Tsumura N.; Miyake Y.: Real-Time Deformations of Organ Based on Structural Mechanics for Surgical Simulators, SPIE:2A1-2A6

[10] Ushiki S.; Matsuguma C.; Koishi T.; Nakaguchi T.; Tsumura N.; Miyake Y.: Real-Time Deformation Model of Liver Based on Structural Mechanics for Medical Training Systems and its Accuracy Evaluation, Asian Forum on Medical Imaging 2007, IEICE Technical Report 106:77-80

[11] Bugdol M. N.; Juszczyk J.: Parametric Curves in Liver Deformation for Laparoscopic Purposes, Information Technologies in Biomedicine 2010, Volume 2

Author:

MSc. Monika Bugdol
Silesian University of Technology
ul. Akademicka 2a
44-100 Gliwice
tel. (032) 237 17 35

email: *monika.bugdol @polsl.pl*